The blazar PKS 0528+134: new results from *Beppo*SAX observations

G. Ghisellini[1], **L. Costamante**[1,2], **G. Tagliaferri**[1], **L. Maraschi**[3], **A. Celotti**[4], **G. Fossati**[5], **E. Pian**[6], **A. Comastri**[7], **G. De Francesco**[8], **L. Lanteri**[8], **C.M. Raiteri**[8], **G. Sobrito**[8], **M. Villata**[8], **I.S. Glass**[9], **P. Grandi**[10], **C. Perola**[11], and **A. Treves**[12]

[1] Osservatorio Astronomico di Brera, V. Bianchi 46, I-23807 Merate, Italy
[2] Univ. di Milano, V. Celoria 16, I-20100 Milano, Italy
[3] Osservatorio Astronomico di Brera, V. Brera 28, I-20100 Milano, Italy
[4] S.I.S.S.A., V. Beirut 2–4, I-34014 Trieste, Italy
[5] CASS/UCSD, La Jolla, CA 92093–0424, USA
[6] TESRE, Bologna, Italy
[7] Osservatorio Astronomico di Bologna, V. Zamboni 33, I-40126 Bologna, Italy
[8] Osservatorio Astronomico di Torino, Strada Osservatorio 20, I-10025 Pino Torinese, Italy
[9] South African Astron. Observ.
[10] IAS/CNR, Frascati, Roma, Italy
[11] University of Rome III, Italy
[12] University of Como, Como, Italy

Abstract. *Beppo*SAX observed 8 times the γ–ray bright blazar PKS 0528+134 in Feb. and Mar. 1997, during a multiwavelength campaign involving EGRET, onboard CGRO, and ground based telescopes. The source was in its faintest X–ray state observed so far, with an unabsorbed [2–10] keV flux of 2.5×10^{-12} erg cm^{-2} s^{-1}. The spectrum can be fitted with a power law, with energy index $\alpha_X = 0.49 \pm 0.07$ between 0.1 and 10 keV. The high energy instrument PDS detected a flux in the 15–100 keV band which appears disconnected from the lower X–ray energies, most likely due to a contaminating source. We consider our findings in the context of the overall spectral energy distribution and discuss their implications for synchrotron and inverse Compton models.

Key words: galaxies: BL Lacertae objects: general – galaxies: BL Lacertae objects: individual: PKS 0528+134 – X-rays: general

1. Introduction

Blazars received an unexpected boost of interest since the discovery, driven by EGRET (and confirmed by OSSE and COMPTEL) that they emit the bulk of their radiative power at γ–ray energies. We are now finding spectral differences among blazars which have already been detected by EGRET. BL Lac objects seem to be characterized by a γ–ray luminosity, L_γ, which is comparable to the luminosity emitted in the rest of the spectrum, while L_γ tends to dominate in blazars with visible broad emission lines. At the same time, the γ–ray dominance correlates with the overall spectral energy distribution (SED) (Comastri et

al. 1997, Fossati et al. 1998). All blazar SED are in fact characterized by two broad emission peaks, believed to be produced by the synchrotron and the inverse Compton processes. The location of these peaks (their frequency and relative flux) is a strong diagnostic tool to discriminate among theoretical models and to find the intrinsic physical parameters of the emitting region (see e.g. Ghisellini et al. 1996; Sikora et al. 1997; Dermer et al. 1997). Examining the SED of γ−ray detected blazars, one finds that both peaks are located at lower frequencies in more powerful, and more γ−ray dominated, sources (Fossati et al. 1998; Ghisellini et al. 1998).

PKS 0528+134, a very powerful blazar, is no exception: its SED shows that the high energy peak is located in the 10–100 MeV range, and the low energy peak between the far IR and the optical bands. For this source, the X–ray band falls near the minimum between the two peaks. Previous X–ray observations by the ASCA satellite showed a flat ($\alpha < 1$, with $F_\nu \propto \nu^{-\alpha}$) spectrum, possibly connecting with the flux in the MeV–GeV band (Sambruna et al. 1997). The uncertainty comes from the paucity of simultaneous observations in both bands, and from the relatively narrow energy windows of the used X–ray detectors. Indeed, if one could join the X–ray and the γ–ray emission with a smooth curve and, more importantly, simultaneous variability were detected, then it would be possible to confidently argue that the emission in both bands is produced by the same mechanism and in the same region.

Furthermore, the fact that the X–ray emission of this source is in a minimum of the SED is of particular interest. In fact, the possible reprocessing of high energy photons, via the creation of electron-positron pairs, leads inevitably to the production of radiation, mainly in the X–ray band. It is therefore crucial to determine how deep this minimum is: a deep minimum would

Send offprint requests to: G. Ghisellini

be a signature that this process *does not* occur (Ghisellini & Madau 1996).

For these reasons we have undertaken a program to observe PKS 0528+134 with the X–ray broad band *Beppo*SAX satellite simultaneously with CGRO (in particular with the EGRET instrument) and other, ground-based, telescopes. In this paper we mainly present the *Beppo*SAX observations, compare them with previous X–ray observations, and construct a simultaneous SED with the optical and EGRET data, briefly discussing our findings.

2. PKS 0528+134

PKS 0528+134 ($z = 2.07$) is one of the most distant quasar detected by EGRET in the γ-ray band. Located in the galactic anticenter region, it is heavily absorbed, although the estimates of A_V are very uncertain (ranging from 2.3 to 5). Thus PKS 0528+134 is faint in the optical, with a typical average magnitude of 19.5 in the V band. It is a strong and flat radio source, with detected superluminal motion ($\beta_{app} \sim$4–6 for $H_0 = 100\,\mathrm{km\,s^{-1}\,Mpc^{-1}}$, Pohl et al. 1996; Britzen et al. 1996). Close to Geminga and the Crab, it was frequently observed by EGRET, and seen flaring in March 1993, when the γ-ray flux was about 6 times brighter than average (Hunter et al. 1993; Mukherjee et al. 1996). Flux changes in the γ-band are accompanied by spectral variations in the sense that the spectrum is harder when brighter (Sambruna et al. 1997; Mukherjee et al. 1997a, 1997b). It is also one of the few extragalactic sources detected by COMPTEL (Collmar et al. 1997; Böttcher & Collmar 1998). The combined COMPTEL and EGRET observations show that the peak of the high energy emission occurs in the MeV band, at least in the flaring state.

3. *Beppo*SAX observations

Between Feb. 21 and March 11, 1997, *Beppo*SAX observed the source 8 times with the narrow field instruments LECS (Low Energy Concentrator Spectrometer; energy range 0.1–10 keV), MECS (Medium Energy Concentrator Spectrometer; energy range 1.3–10 keV) and PDS (Phoswich Detector System; energy range 15–200 keV) (Boella et al. 1997).

In Table 1 we report the journal of observations, with the corresponding exposure times and derived net count rates.

4. Results

4.1. Light curves

We have extracted light curves from the data of the three MECS units (merged together) using XSELECT and considering a circle of radius $4'$ centered around the target. In Fig. 1 we show the total MECS count rates obtained with the XIMAGE program corresponding to the 8 observations. This light curve is consistent with a constant. We can set an upper limit on the amplitude of possible variations of $\sim$40%. No significant variations are present within the single observations either.
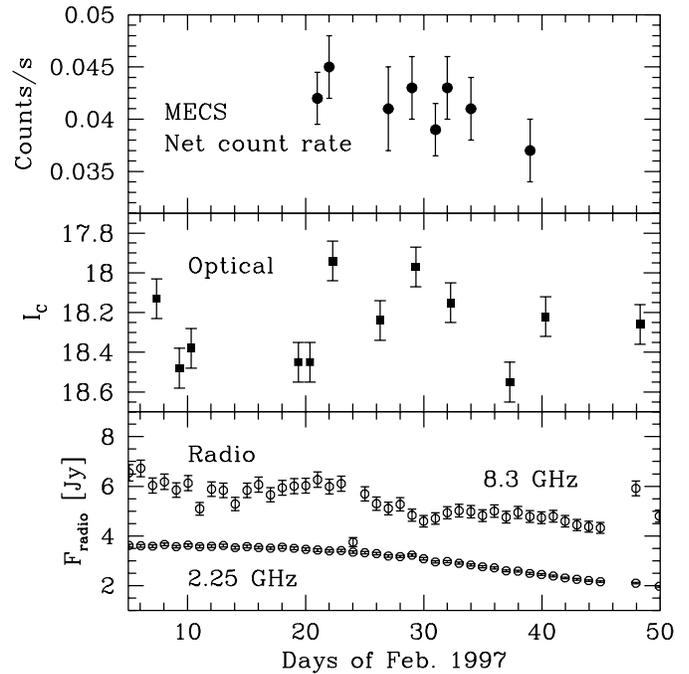

Fig. 1. The top panel shows the MECS light curve, corresponding to the 8 observations. In the middle panel we report the optical light curve in the same period, in the I_C filter. The bottom panel shows the light curve at 8.3 and 2.25 GHz, by the Green Bank monitoring campaign.

Simultaneously with the *Beppo*SAX observations, the source was observed in the optical, with the REOSC 1.05 meter telescope of Pino Torinese (see Villata et al. 1997 for a description of the instrument and the data analysis procedure), and in the radio band with the Green Bank Interferometer (GBI). As shown by the middle and lower panels of Fig. 1, the source was varying significantly in the optical (with a probability $> 99.9\%$) and at 8.3 GHz.

We also observed the source in the near infrared with the 1.9 m telescope at Sutherland using the MkIII photometer, obtaining $K = 14.76 \pm 0.23$ on Mar 2, 1998 (JD=2450510), using a $12''$ diameter aperture.

4.2. Spectral fitting

4.2.1. LECS and MECS

Spectra of the LECS and MECS detectors have been extracted using XSELECT and a circle of radius $4'$ around the target for both the instruments (given the weak flux of the source and the heavy absorption under 0.7 keV, we have not used the $8.5'$ radius recommended for the LECS for brighter sources, to minimize the effects of the background, especially at low energies). As suggested by the Science Data Center of *Beppo*SAX (SDC), after checking that the background was constant during the observations, we have subtracted the background using the blank sky fields selecting the same detector regions where the target is located. We used the response matrices released by the SDC in September 1997. The LECS and MECS spectra have been

Table 1. *Beppo*SAX observation log

Date	Start[1]	End[1]	LECS[2]	net cts s^{-1}	MECS[2]	net cts s^{-1}	PDS[2]	net cts s^{-1} [3]
Feb 21	02:17:38	09:08:06	6322	0.015±0.007	14487	0.042±0.002	6919	0.22±0.08
Feb 22	23:29:16	06:48:06	5046	0.014±0.007	13365	0.045±0.003	5925	0.24±0.08
Feb 27	14:38:39	19:18:11	3945	0.011±0.010	6917	0.041±0.004	1622	0.28±0.17
Mar 1	00:52:14	07:43:06	4261	0.012±0.010	13547	0.043±0.003	6344	0.29±0.08
Mar 3	01:38:02	08:28:06	5053	0.015±0.007	14241	0.039±0.002	6783	0.16±0.08
Mar 4–5	21:53:08	04:28:05	2793	0.015±0.010	11254	0.043±0.003	4914	0.11±0.09
Mar 6–7	21:03:14	03:53:05	3083	0.012±0.010	12762	0.041±0.003	5587	0.26±0.09
Mar 11	00:17:06	06:06:05	2497	0.012±0.011	11490	0.037±0.003	5374	0.29±0.09
Total			32998	0.014±0.001	98063	0.041±0.001	43468	0.23±0.03

[1] UT Time; [2] Exposure time in seconds; [3] values in the entire PDS band

jointly fit after allowing for a constant rescaling factor of 0.9 for the LECS data (this factor accounts for uncertainties in the inter–calibration of the instruments; Fiore, priv. comm.).

Fitting the 8 observations separately with a single power law and free hydrogen column density, N_H, gives consistent values, within the (rather large) uncertainties. We therefore decided to combine the 8 spectra, in order to increase the signal to noise ratio. A single power law fit to the LECS+MECS dataset (see Fig. 2) yields an energy spectral index $\alpha_x = 0.48 \pm 0.11$ with $N_H = (5.0 \pm 1.9) \times 10^{21}$ cm^{-2} (unless otherwise indicated, the errors from the fits are at 90% confidence level, for two parameters of interest). No spectral feature is required by the fit and in particular an upper limit of $EW < 200$ eV can be set to the equivalent width (in the source frame) of the 6.4 keV fluorescence K_α iron line (see Sect. 5.1 for more discussion). The results of the spectral fitting are reported in Table 2.

As mentioned in the Introduction, the value of the N_H column density is uncertain, yet its determination is important, since the knowledge of the corresponding optical extinction allows to determine the location of the synchrotron peak. *Beppo*SAX data, alone, cannot well constrain N_H, due to the faint level of the source. PKS 0528+134 was instead much brighter during the ASCA observations of March 1995, allowing a better determination of the N_H column [$N_H = 5.3(\pm 0.3) \times 10^{21}$ cm^{-2}], as described in Sect. 5.1.

Since the *Beppo*SAX measurement of the N_H column is consistent with the value found by ASCA, we fixed the N_H at the latter value. In this case the LECS+MECS data can be modeled by a single power law with an energy index $\alpha_x = 0.49 \pm 0.07$ (90% confidence level for one parameter of interest).

4.2.2. PDS

Source visibility windows were selected following the criteria of no earth occultation and high voltages stability during the exposures. In addition, the observations closest to the South Atlantic anomaly were discarded from the analysis. From collimators positions the ON and OFF time windows were also created and merged with the source visibility window to create the final time windows on which the source+background and background spectra were accumulated for each of the four

PDS units, using the XAS software package. A filtering for the temperature and energy dependence of the pulse rise time was used.

The source was significantly detected up to ~90 keV. For each pointing, the grouped spectra from the four units were coadded. The net count rates are reported in Table 1.

To increase the S/N, we have averaged the eight PDS spectra and binned the resulting spectrum in 4 energy intervals. For the fitting, we used the response matrix available at SDC, keeping the rescaling factor with respect to the MECS constant and equal to 0.85 (this factor allows for uncertainties in the inter–calibration of the instruments).

As shown in Fig. 2, the PDS data points lie above the model fit for the LECS and MECS datasets. In particular, including the PDS data and using a single power law fit with N_H fixed to the value found by ASCA, we obtain $\alpha_x = 0.42 \pm 0.06$, with the PDS points still lying above the fit (see Table 2 for details).

The same three datasets (LECS+MECS+PDS) were also fitted with a broken power law model with $\alpha_1 = 0.48 \pm 0.06$ and $\alpha_2 = -0.15 \pm 0.14$ and break energy $E_{break} \sim 9^{+3}_{-2}$ keV, leading to a $\chi_r^2 = 1.34$ for 57 d.o.f. This model significantly improves the fit, according to the F–test ($> 99.5\%$), but the χ^2–value yields a probability less than 5% that the model is correct. A power law fit to the PDS data alone gives a spectral index $\alpha_x = 0.82 \pm 0.35$.

As can be seen, the high energy flux detected by the PDS shows a clear discontinuity with respect to the LECS/MECS data. A possible explanation can be that the PDS data are contaminated by the presence of another source in its field of view. The PDS field of view is ~1.3 degree, with no imaging capability. The response matrix of this instrument is triangular, with a flat top of 3$'$ and a reduction of a factor 2 in sensitivity at 38$'$ from the center (Frontera et al. 1997). The MECS have a field of view of radius 30$'$, and there are no sources other than PKS 0528+134 detected at more than 3σ.

We checked the ROSAT PSPC WGA catalog (White et al. 1994) for sources at an angular distance < 1 degree from PKS 0528+134. There are two unidentified sources (1WGA J0532.9+134, at a distance of 31 arcmin from PKS 0528+134, and 1WGA J0533+135, at 41 arcmin) with a count rate in the ROSAT band comparable to that of PKS 0528+134. No sources
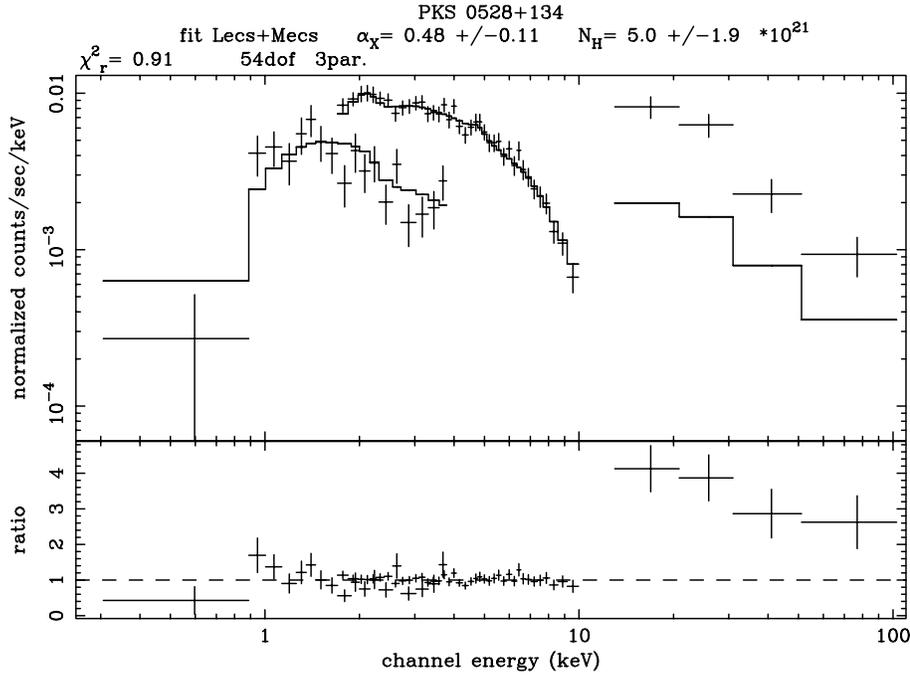
Fig. 2. Fit to the LECS and MECS *Beppo*SAX spectrum. PDS data are not used for the fit, and appear to lie above the extrapolation of the power law from lower energies.

Table 2. Fits to *Beppo*SAX Data: single power law

α	N_H 10^{21} cm^{-2}	$F_{[2-10\ \text{keV}]}$ erg/cm^2 s^{-1}	χ^2_r	d.o.f.	$F_{1\ \text{keV}}$ μJy	Notes
0.48±0.11	5.0±1.9	2.53e-12	0.91	54	0.29±0.05	LECS+MECS, free N_H
0.49±0.07	5.3	2.54e-12	0.91	55	0.30±0.03	LECS+MECS, fixed N_H
0.37±0.11	3.9±1.6	2.59e-12	1.71	58	0.24±0.04	LECS+MECS+PDS, free N_H
0.42±0.06	5.3	2.60e-12	1.74	59	0.27±0.03	LECS+MECS+PDS, fixed N_H

Table 3. Single power law fits to ASCA data with fixed N_H

α	$F_{[2-10\ \text{keV}]}$ erg cm^{-2}s^{-1}	χ^2_r	d.o.f.	$F_{1\ \text{keV}}$ μJy	Date
0.66±0.06	3.77e-12	0.89	93	0.57±0.05	28 Aug 1994
0.71±0.04	9.55e-12	1.21	100	1.57±0.07	7 Mar 1995
0.71±0.04	10.62e-12	1.18	69	1.76±0.07	14 Mar 1995
0.72±0.03	13.80e-12	0.91	140	2.32±0.07	19 Mar 1995

Fits to the summed ASCA data of March 95

α_1	α_2	E_{break} keV	N_H 10^{21} cm^{-2}	$F_{[2-10\ \text{keV}]}$ erg/cm^2 s^{-1}	χ^2_r	d.o.f.	Notes
0.72±0.04	-	-	5.3±0.3	1.15e-11	1.13	207	free N_H, single power law
0.00±0.16	0.65±0.03	1.47 ± 0.10	3.9 fix	1.15e-11	1.08	206	fixed N_H, broken power law

were instead found in the EXOSAT and ASCA public archives. Given the low galactic latitude of PKS 0528+134 and the large offset of the PDS data points with respect to the extrapolation of the MECS spectrum, we think that the PDS data might be contaminated by other sources. For this reason, in the discussion of the SED of PKS 0528+134, we will not consider the PDS spectrum.

5. Comparison with previous observations

5.1. ASCA observations

As already mentioned, a long standing problem with this source is the determination of its optical extinction and the column N_H along the line of sight. The value that we found with the *Beppo*SAX observations is in agreement with the sum of the estimated absorption caused by the column of neutral galactic hydrogen [$N_H = (2.6 \pm 0.1) \times 10^{21}$ cm^{-2}], plus that due to
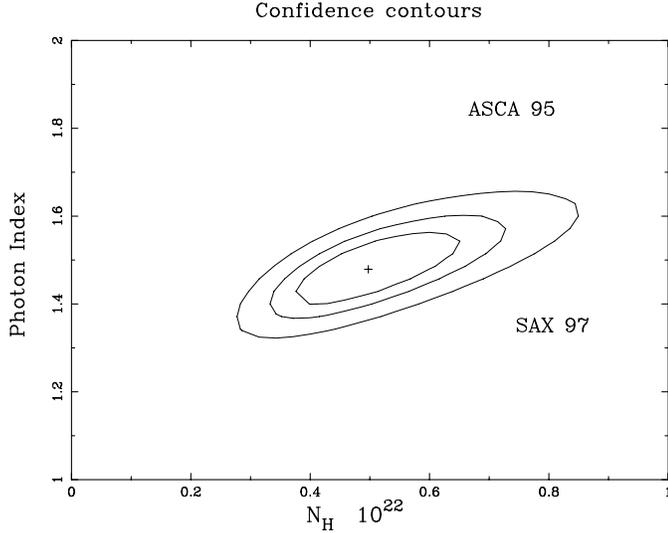
Fig. 3. Confidence contours (68%, 90% and 99%) for fits with a single power law plus absorption for the sum of the three August 1995 ASCA observations and the sum of the eight *Beppo*SAX observations.
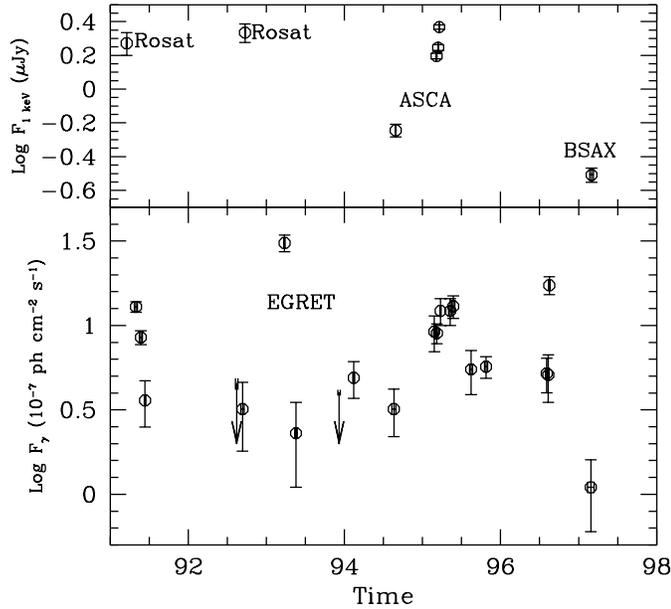

Fig. 4. Historical light curves in the X–ray and γ–ray bands, after 1991. All X–ray data have been reanalysed assuming a fixed $N_{\rm H} = 5.3 \times 10^{21}\,{\rm cm}^{-2}$.

the outer edge of the molecular cloud Barnard 30 in the λ Orion rings of clouds, $[N_{\rm H} \sim 1.3 \times 10^{21}\,{\rm cm}^{-2}]$ (Sambruna et al. 1997).

In March 1995, ASCA observed PKS 0528+134 three times, within 2 weeks, during an active state of the source. The last of these observations was analyzed by Sambruna et al. (1997), finding a best fit value of $N_{\rm H} = (5.57 \pm 0.4) \times 10^{21}\,{\rm cm}^{-2}$, in good agreement with the value found in our *Beppo*SAX observations. The entire set of the three observations was instead analyzed by Kubo et al. (1998), but assuming a column density fixed at the neutral galactic hydrogen value $[N_{\rm H} =$

$(2.6 \pm 0.1) \times 10^{21}\,{\rm cm}^{-2}]$, without considering the extra absorption due to the Barnard cloud.

We therefore decided to re–analyze the full ASCA data set. We first fitted the 3 observations separately, finding that, despite a flux change of a factor 1.5, the three best fit values of the spectral index were nearly equal: with free $N_{\rm H}$ the values were within the 68% confidence uncertainties. We then fitted the sum of the 3 ASCA observations and the increased signal–to–noise ratio allowed to obtain the best measure of the column so far: $N_{\rm H} = (5.3 \pm 0.3) \times 10^{21}\,{\rm cm}^{-2}$ (see Table 3 for the fit parameters).

In Fig. 3 we show the confidence contours in the photon index–column plane, for the sum of the August 1995 ASCA observations and the sum of the 8 *Beppo*SAX observations.

We also searched for the possible presence of an Fe K_α line at 6.4 keV, finding an upper limit to its equivalent width of 67 eV in the summed 1995 spectrum (calculated in the rest frame of the source). This limit is only marginally consistent with the value of $EW = 119 \pm 58$ eV reported by Reeves et al. (1997) analyzing the 1994 ASCA spectrum, when the source was fainter.

5.2. Historical X–ray and γ–ray light curves

In order to understand the relationship between X–ray and γ–ray emission, we compared both the light curves in the last 7 years and the spectral indices behaviour in these two bands.

In Fig. 4 (upper panel) we show the light curves of all the observations in the X–ray band after 1991. For consistency, we have re–analyzed all these data (taken from the archives) with the same $N_{\rm H} = 5.3 \times 10^{21}\,{\rm cm}^{-2}$. In 1995 the source varied by 50% in 2 weeks. Between the 1995 ASCA and our 1997 *Beppo*SAX observations, when the source was at its faintest historical level, the flux decreased by a factor $\sim$7. The lower panel shows the light curve of the γ–ray flux, as observed by EGRET (Mukherjee et al. 1996, 1997a, 1997b). In γ–rays the source was observed more often, with a variability of a factor 13 in 2 months, and a factor $\sim$2 in 2 days during the 1993 flare (see Mukherjee et al. 1996).

The lack of simultaneity of previous observations and the paucity of X–ray data do not allow to establish any (or absence of) correlation. It should be however noticed that for the three epochs of simultaneous observations (Aug. 1994, Mar. 1995 and Feb.–Mar. 1997), the X–ray and γ–ray flux levels follow the same trend.

5.3. Flux–spectral index correlations?

In Fig. 5 (upper panel) we report the X–ray spectral indices determined by *Beppo*SAX and ASCA data vs the 1 keV flux. While all ASCA points are consistent with the same spectral index, the spectral shape determined by *Beppo*SAX observations is significantly flatter (see also Fig. 3), and corresponds to the fainter flux.

In the lower panel of Fig. 5 we show the γ–ray spectral index as a function of the γ–ray flux (data from Mukherjee et al. 1996,
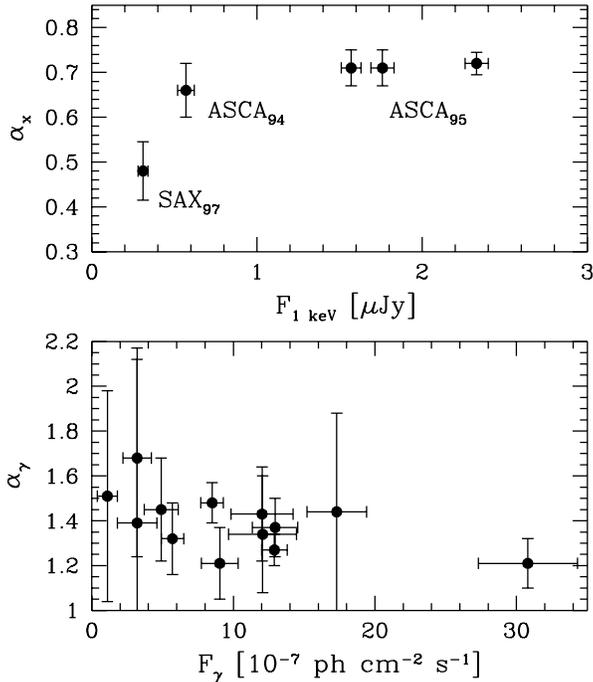
Fig. 5. Spectral indices vs flux in the [2–10] keV and [0.05–1] GeV bands. All X–ray data have been reanalysed assuming a fixed $N_{\mathrm{H}} = 5.3 \times 10^{21}$ cm^{-2}. γ–ray data from Mukherjee et al. 1996, 1997a, 1997b, 1999.

1997a, 1997b, 1999). The large error bars of α_γ, especially at faint fluxes, do not allow any conclusion about the presence of a trend: although the linear correlation coefficient is $\sim$–0.6 (random probability=0.02), a χ^2–test on a fit with a constant gives 15% probability that the two quantities are not correlated.

Although we cannot draw any firm conclusion about the flux–spectral index correlations, note that during the *Beppo*SAX observations the source, in its faintest state, had the flattest spectral index. This is an unusual behavior for blazars (even if some other example exist, see Ulrich et al. 1997), and likely to yield important information and/or constraints on the emission models, as discussed below.

6. The SED

In Fig. 6 we show the overall spectral energy distributions of PKS 0528+134 at different epochs, as indicated by the labels. Data have been dereddened assuming $N_{\mathrm{H}} = 5.3 \times 10^{21}$ cm^{-2}, corresponding to $A_V = 3$. We have reported the minimum and maximum values of the radio and optical data obtained during our campaign.

The not simultaneous data shown in Fig. 6 have been taken from Wall & Peacock 1985; Bloom et al. 1994; Edelson 1987; Reuter et al. 1997; Rieke et al. 1982; Condon et al. 1977; Collmar et al. 1997; McNaron-Brown et al., 1995 and Mukherjee et al. 1996. We also show some simultaneous sets of data: the 1991 Comptel and EGRET spectrum (Collmar et al. 1997); the 1994 and 1995 X–ray (ASCA) and EGRET data (we also have an optical point during the 1994 campaign; data for these two

campaigns are presented in Sambruna et al. 1997 and references therein); our 1997 IR, optical, X–ray data together with the EGRET point from Mukherjee et al. 1997b and the radio data from the GBI archive (see Fig. 1).

As all other γ–ray bright blazars, also the SED of PKS 0528+134 is characterized by two peaks, one between the far IR and optical spectral bands, and the other at MeV energies. As discussed in Sambruna et al. (1997), the dereddened (using $A_V = 3$) optical spectrum is inverted ($\alpha_o = -0.18 \pm 0.08$), and thus indicative of the presence of a 'blue bump' component. This is not easy to reconcile with the very large and rapid optical variability. We also note that due to the presence of molecular clouds along the line of sight the gas to dust ratio may be anomalous and the value of A_V may be larger than the one adopted above. Further spectral observations in the IR optical range could help clarifying this issue.

As can be seen, the MeV–GeV emission dominates the bolometric output by a large amount, reaching an (isotropic) luminosity in excess of 10^{49} erg s^{-1} (with $H_0 = 50$ km s^{-1} Mpc^{-1} and $q_0 = 0.5$).

7. Discussion

Among the models proposed to account for the blazar γ–ray emission, the most accredited are those based on the Inverse Compton process, between the relativistic electrons responsible for the synchrotron emission and seed photons which can either be the synchrotron photons themselves [synchrotron–self Compton (SSC)] or photons produced externally to the jet (EC) (Maraschi et al. 1992; Bloom & Marscher 1993; Sikora et al. 1994, Dermer et al. 1992; Blandford & Levinson 1995; Ghisellini & Madau 1996).

In all cases synchrotron radiation is responsible for the low energy emission (up to the optical-UV band), and the inverse Compton process gives rise to the X– to γ-ray spectrum. Seed photons of different origin may well coexist and their relative contribution in the same object may be different in different states and in different energy bands. The presence of luminous emission lines and possibly of a blue bump indicates, in the case of PKS 0528+134, that photons outside the jet should play an important role in the IC process (EC scenario). For a detailed discussion of the fitting of the 1994 overall spectrum with SSC and EC models see Sambruna et al. (1997).

As shown in Fig. 6, the source shows correlated X–ray and γ–ray flux variability. In particular, during the 1997 campaign, the source was at its faintest level both in X– and γ–rays. In this occasion, the X–ray spectrum was significantly flatter than in higher states. This is in contrast with the "flatter when brighter" behavior of blazars (Ulrich et al. 1997), and therefore likely to give important constraints on the emission models.

Within the framework of the SSC and EC model we can envisage two scenarios to explain the observed behavior:

1) The X–rays are produced by *both* the self–Compton and EC processes. Therefore there can be *two* typical frequencies of the seed photons: one corresponding to the peak of the synchrotron emission (in the far IR), and one corresponding to the exter-
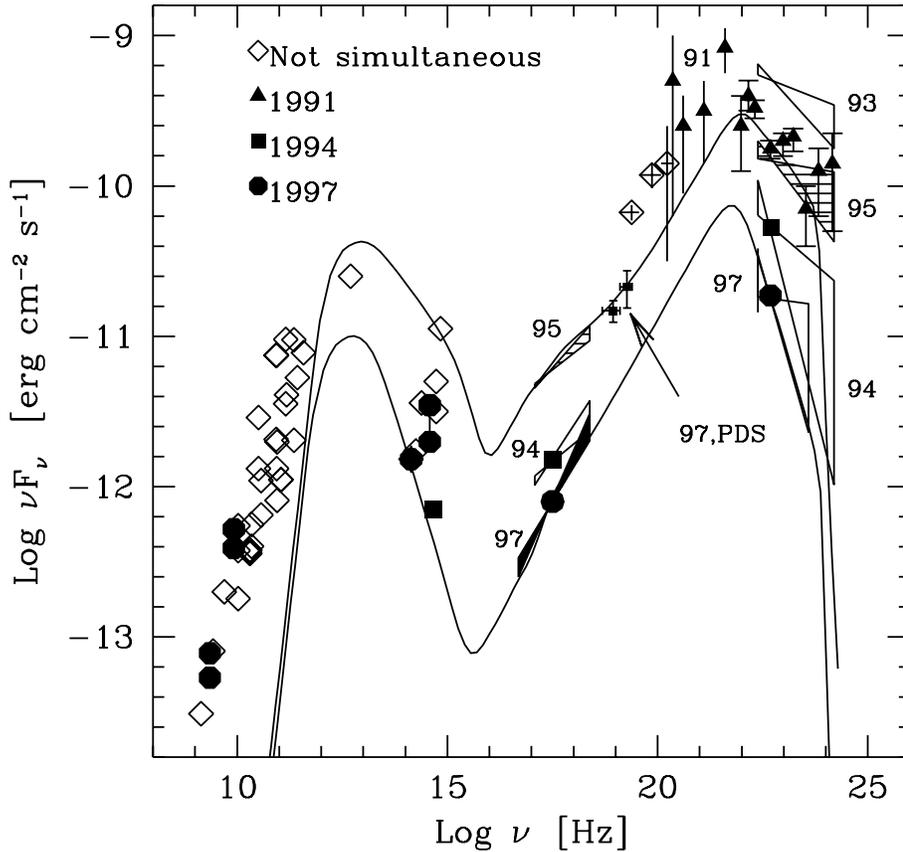
Fig. 6. Overall spectral energy distribution of PKS 0528+134. Simultaneous observations are indicated by the different marks, as labeled. Other non–simultaneous data are taken from the literature (see text). The solid line is a fit to the 1997 spectrum made with a homogeneous, one–zone model, corresponding to a source with a size $R = 5 \times 10^{16}$ cm, a magnetic field $B = 8.6$ Gauss, in which beaming corresponds to a Doppler factor $\delta = 17$. Relativistic electrons are injected continuously throughout the source, at a rate corresponding to an intrinsic luminosity $L' = 3.7 \times 10^{44}$ erg s^{-1}, with a power law spectrum $\propto \gamma^{-3.8}$ between $\gamma_1 = 200$ and $\gamma_2 = 3000$. In this case the EC component dominates the entire high energy band. The fit to the 1995 spectrum is obtained adopting the same R, δ and B, but with a larger injected power of $L' = 1.8 \times 10^{45}$ erg s^{-1} and with a flatter injected electron spectrum ($\propto \gamma^{-2.7}$) between $\gamma_1 = 200$ and $\gamma_2 = 4000$. In this case both the SSC and the EC components contribute to the low energy X–ray spectrum, while only the EC component contributes above a few tens of keV. Note that the shown PDS points lie above the extrapolation from the spectrum in the LECS and MECS band. Given the possibility of contaminating sources (see text), we do not consider these points when applying the model.

nal radiation. In the case that the emission lines and blue bump photons form the bulk of the external radiation, their typical frequency, as observed in the comoving frame, is in the far UV. If the radiation energy densities of these two components are comparable (within a factor 10), then the self–Compton emission would dominate at lower X–ray energies, while the EC spectrum would be entirely responsible for the emission in the γ–ray band. This is because the self–Compton spectrum is somewhat steeper than the EC one produced by the same electrons, and because the maximum self–Compton frequency is lower. Let us suppose now that the number of emitting electrons increases. In this case the synchrotron and the EC fluxes vary linearly, while the self–Compton one varies quadratically, making the SSC component to dominate the flux over a larger X–ray energy range.

We have reproduced the 1997 "low state" and the 1995 "high state" spectra along these lines, with a homogeneous one–zone model, taking into account both the SSC and the EC contribu-

tions to the high energy spectra. The model finds the equilibrium (steady state) electron distribution by balancing the injection of relativistic particles and their radiative cooling. Photon–photon collisions and electron–positron pair production, Klein–Nishina effects on the scattering cross section and Coulomb collisions are taken into account (see Sambruna et al. 1997 for further details). The input parameters are given in the caption of Fig. 6. We "fitted" both spectra leaving the dimension and the beaming factor of the source unchanged, as well the low energy cut-off of the injected electron distribution. We have instead increased by a factor 3 the injected power in the high state, also characterized by a slightly flatter injected electron distribution. The resulting spectra, shown in Fig. 6, reproduce quite well the different X and γ–ray slopes.

2) Another process that can in principle account for a flatter X–ray spectral index when the source is fainter, is e$^{\pm}$ pair production. When the source is in a high (and hard) γ–ray state, a small fraction of the high energy power could be converted in

electron–positron pairs via $\gamma - \gamma$ interaction with X–ray photons. This process produces a steepening of the electron spectrum towards lower energies, yielding a brighter and steeper IC spectrum in the X–ray band. The main difficulty with this scenario is the fine tuning required in the amount of the high energy power that is absorbed and reprocessed, which must be of the order of a few per cent. If it is less, then pairs are not produced in a sufficient amount to contribute anywhere in the emitted spectrum. If it is higher, then they could increase the number of target photons for γ–γ collisions, inducing a catastrophic cascade, and an overproduction of X–ray with respect to what we observe (Svensson 1987).

For these reasons, we conclude that the required moderate pair reprocessing is unlikely to occur in this source.

8. Summary and conclusions

From the analysis of the *Beppo*SAX and ASCA data, and from the construction of the simultaneous SED of the source at different epochs we find:

– *Beppo*SAX observed PKS 0528+134 in its faintest X–ray state, characterized by the flattest X–ray spectrum, of energy index $\alpha_x = 0.49 \pm 0.07$.
– The three ASCA observations of March 1995, despite the different fluxes, are characterized by the same spectral index $\alpha_x = 0.71 \pm 0.04$. Fitting the sum of these data allows to determine with improved precision the absorbing hydrogen column density of the source, $N_{\rm H} = (5.3 \pm 0.3) \times 10^{21}\,{\rm cm}^{-2}$, which corresponds to an optical absorption of $A_V = 3 \pm 0.17$.
– The overall simultaneous SED follows the general trend of blazars, as found by Fossati et al. (1998). In fact the SED is characterized by two peaks, in the mid or far infrared and in the MeV band, respectively, as for the most luminous blazars. Furthermore the γ–ray luminosity dominates the overall power output during active states, again in agreement with the general behavior of other powerful blazars (see e.g. von Montigny et al., 1995).
– We have fitted the 1995 SED (high state) and the 1997 SED (low state) with a homogeneous model, in which the emission from the far IR to the UV is produced by the synchrotron process, and the high energy flux is due to the sum of the synchrotron self–Compton and the external Compton contributions. The former becomes more important (in the X–ray band) for increasing source power. This accounts for the unusual observed X–ray behavior (flatter state when the source was fainter). Variations of the γ–ray flux and spectral shape might be explained by a flattening of the high energy part of the electron distribution.

References

Blandford R.D., Levinson A., 1995, ApJ 441, 79
Bloom S.D., Marscher A.P., Gear W.K., et al., 1994, AJ 108, 398
Bloom S.D., Marscher A.P., 1993, In: Friedlander M., Gehrels N. (eds.) Proceeedings of the Compton Symposium. AIP, New York, 578
Boella G., Butler R.C., Perola G.C., et al., 1997, A&AS 122, 299
Böttcher M., Collmar W., 1998, A&A 329, L57
Britzen S., Witzel A., Krichbaum T., 1996, In: Kirk J.G., Camenzind M., von Montogny C., Wagner S. (eds.) Gamma–ray emitting AGN. MPI H – V37, p. 109
Collmar W., Bennet K., Bloemen H., et al., 1997, A&A 328, 33
Comastri A., Fossati G., Ghisellini G., Molendi S., 1997, ApJ 480, 534
Condon J.J., Hicks P.D., Jauncey D.L., 1977, AJ 82, 692
Dermer C.D., Sturner S.J., Schlickeiser, R., 1997, ApJS 109, 103
Dermer C.D., Schlickeiser R., Mastichiadis A., 1992, A&A 256, L27
Edelson R., 1987, AJ 94, 1150
Fossati G., Maraschi L., Celotti A., Comastri A., Ghisellini G., 1998, MNRAS 299, 433
Frontera F., Costa E., Dal Fiume D., et al., 1997, Proc. SPIE 3114, 206
Ghisellini G., Madau P., 1996, MNRAS 280, 67
Ghisellini G., Celotti A., Fossati G., Maraschi L., Comastri A., 1998, MNRAS 301, 451
Ghisellini G., Maraschi L., Dondi L., 1996, ApJS 120, 503
Hunter S.D., Bertsch D.L., Dingus B.L., et al., 1993, ApJ 409, 134
Kubo H., Takahashi T., Madejski G., et al., 1998, ApJ 504, 693
Maraschi L., Ghisellini G., Celotti A., 1992, ApJ 397, L5
McNaron-Brown K., Johnson W.N., Jung G.V., et al., 1995, ApJ 451, 575
Mukherjee R., Dingus B.L., Gear W.K., et al., 1996, ApJ 470, 831
Mukherjee R., Bertsch D.L., Bloom S.D., et al., 1997a, ApJ 490, 116
Mukherjee R., Bertsch D.L., Bloom S.D., et al., 1997b, In: Dermer C.D., Strickman M.S., Kurfess J.D. (eds.) Proceedings of the Fourth Compton Symp. Williamsburg, VA AIP Conference Proceedings 410, p. 1346
Mukherjee R., Boettcher M., Hartman R.C., et al., 1999, ApJ, submitted (astro-ph/9901106)
Pohl M., Reich W., Schlickeiser R., Reich P., Ungerechts H., 1996, A&AS 120, 529
Reeves J.N., Turner M.J.L., Ohashi T., Kii T., 1997, MNRAS 292, 468
Reuter H.-P., Sievers A., Paubert G., et al., 1997, A&AS 122, 271
Rieke G.H., Lebofsky M.J., Wiśniewski W.Z., 1982, ApJ 263, 73
Sambruna R.M., Urry C.M., Maraschi L., et al., 1997, ApJ 474, 639
Sikora M., Begelman M.C., Rees M.J., 1994, ApJ 421, 153
Sikora M., Madejski G., Moderski, R., Poutanen J., 1997, ApJ 484, 108
Svensson R., 1987, MNRAS 227, 403
Ulrich M.-H., Maraschi L., Urry C.M., 1997, ARA&A 35, 445
Villata, M., Raiteri C.M., Ghisellini G., et al., 1997, A&AS 121, 119
von Montigny C., Bertsch D.L., Chiang J., et al., 1995, ApJ 440, 525
Wall J.V., Peacock J.A., 1985, MNRAS 216, 173
White N.E., Giommi P., Angelini L., 1994, IAUC 6100